Fluorophore Design

Deutsche Ausgabe: DOI: 10.1002/ange.201506429
Internationale Ausgabe: DOI: 10.1002/anie.201506429

Rational Improvement of Molar Absorptivity Guided by Oscillator Strength: A Case Study with Furoindolizine-Based Core Skeleton

*Youngjun Lee, Ala Jo, and Seung Bum Park**

Abstract: *The rational improvement of photophysical properties can be highly valuable for the discovery of novel organic fluorophores. Using our new design strategy guided by the oscillator strength, we developed a series of full-color-tunable furoindolizine analogs with improved molar absorptivity through the fusion of a furan ring into the indolizine-based Seoul fluorophore. The excellent correlation between the computable values (oscillator strength and theoretical S_0–S_1 energy gap) and photophysical properties (molar absorptivity and emission wavelength) confirmed the effectualness of our design strategy.*

Molar absorptivity (ε) is an intrinsic property of every chemical entity, and it represents how well the entity absorbs light at any given wavelength.[1] From a synthetic point of view, the development of a new design strategy that allows for the predictable enhancement of the molar absorptivity of a species is highly valuable—with benefits spanning from aiding in the development of light-harvesting materials, such as dye-sensitized solar cells (DSSC), to various types of fluorescent materials.[2] However, very few research articles have reported the successful improvement of molar absorptivity of particular initial compounds[3] because the prime strategy, an extension of the π-conjugated systems of these compounds, does not always guarantee increased molar absorptivity, and some instances have even been shown to have negligible or opposite effects.[4] To the best of our knowledge, there was no scientific report pursuing the rational design of organic fluorophores with enhanced molar absorptivity.

Fluorescent organic dyes are a class of emissive materials with high sensitivity, selectivity, accessibility, and ease of use, making them first-class monitoring tools in molecular biology and life sciences.[5] However, only a limited number of fluorophores, such as cyanine, BODIPY (BODIPY = boron-dipyrromethene), fluorescein, and rhodamine, have been repeatedly used in the majority of research studies, mainly owing to their innate brightness, which in turn is associated with their excellent molar absorptivity.[6] Therefore, a rational improvement of molar absorptivity is in high demand for the development of distinctive organic fluorophores in various practical uses. To address this issue, we hypothesized that molar absorptivity of organic fluorophores can be rationally improved by the guidance of a computable value, the oscillator strength (or f value).[1,7] Oscillator strength is a physical parameter that shows the allowedness in the radiative electron transition of molecules and can be tuned through the incorporation of various functional groups.[9] To test this hypothesis, starting from Seoul fluorophore (SF), an indolizine-based fluorescent core skeleton,[10] we envisioned the development of a novel core skeleton with improved photophysical properties by the enhancement of its molar absorptivity, guided by the computable oscillator strength value. We previously observed a marginal enhancement of molar absorptivity when we tried the incorporation of naphthyl or styryl groups in SF (see Figure S1 in the Supporting Information).[11] Therefore, we focused on the introduction of a heteroaromatic ring fused in indolizine core itself to extend the π-conjugated system, because the electronic nature of initial fluorophores can be significantly transformed by the inductive or resonance effects of the newly introduced heteroatom.[12]

Of the potential heteroaromatic rings, we decided to fuse a furan, after considering the remarkable molar absorptivity enhancement of BODIPY reported by Suzuki and co-workers.[13] Given that the SF system is based on the lactam-embedded indolizine moiety, combining a furan ring with the indolizine of SF can generate six different furoindolizine isomers, depending on the fused position between the five- and six-membered rings and the arrangement of the atomic oxygen in the furan (Figure 1). Without any challenging or time-consuming efforts to synthesize all possible candidates, we performed time-dependent density functional theory (TD-DFT) calculations at B3LYP/6-31G* level to obtain the oscillator strength values of the six isomers, thereby estimating the degree for which the electron transition from the S_0 to

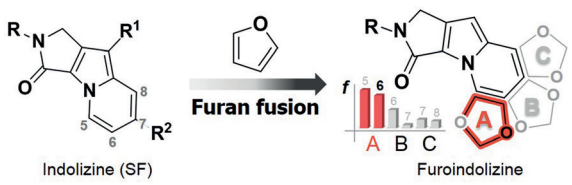

Figure 1. Chemical structures of novel furoindolizine-based fluorophores and their calculated oscillator strength values (f values) using TD-DFT calculation at B3LYP/6-31G* level. The R group represents an aliphatic linker moiety.

[*] Y. Lee, A. Jo, Prof. Dr. S. B. Park
Department of Chemistry, Seoul National University
Seoul 151-747 (Korea)
E-mail: sbpark@snu.ac.kr

Supporting information for this article is available on the WWW under http://dx.doi.org/10.1002/anie.201506429.

© 2015 The Authors. Published by Wiley-VCH Verlag GmbH & Co. KGaA. This is an open access article under the terms of the Creative Commons Attribution Non-Commercial NoDerivs License, which permits use and distribution in any medium, provided the original work is properly cited, the use is non-commercial and no modifications or adaptations are made.

the S_1 state of each core skeleton is allowed (see Table S1). This result indicates that placing the furan at the "A" position would have the highest *f* value, potentially implying the highest molar absorptivity. Of the two cores at "A", we finally selected "A-6" to generate an unprecedented furoindolizine core skeleton for the in-depth study of structure and photophysical properties (SPPR), owing to its greater synthetic accessibility.

To construct a library set covering a wide range of molar absorptivity and emission wavelengths, we strategically chose the positions for the incorporation of the R^1 and R^2 groups, as based on the quantum-mechanical calculations. First, the R^1 position was selected on the basis of the electron density in the highest occupied molecular orbital (HOMO) in comparison with that in the lowest unoccupied molecular orbital (LUMO), using TD-DFT calculations (Figure 2 a). Following

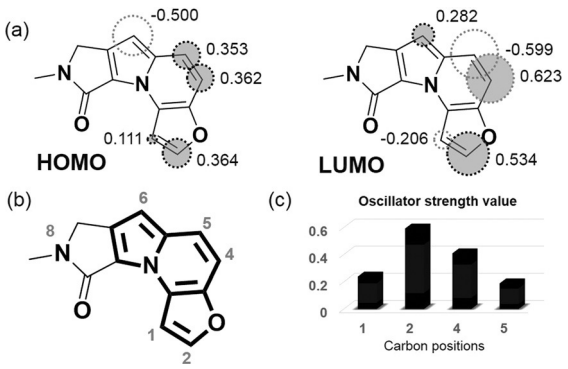

Figure 2. A design principle for selecting the functional group positions in the furoindolizine skeleton. a) The atomic coefficients in HOMO and LUMO of the core skeleton. b) Chemical structure of lactam-embedded furo[3,2-*e*]indolizine core skeleton. c) Calculated oscillator strength *f* values of the S_0–S_1 transition when incorporated with the phenyl group at each carbon position.

our previous studies,[10b] we hypothesized that the electron-donating group (EDG), existing on the carbon with the much larger atomic coefficient in HOMO than that in LUMO, would induce a smaller energy gap—bathochromic shifts of fluorescence emission wavelength—as it would preferentially elevate the energy level of the HOMO over that of the LUMO (Figure S2).[14] In the same manner, the electron-withdrawing group (EWG), existing on the carbon with the larger atomic coefficient in the LUMO, would induce selective reduction of the energy level of the LUMO, causing a smaller energy gap. Accordingly, we selected the C6 atom as the position for the R^1 group, leaving the C2, C4, and C5 atoms as potential sites for the R^2 group (Figure 2 b). Next, the latent R^2 position was carefully assessed by the calculated oscillator strength values to enhance their molar absorptivity. As shown in Figure 2 c, it was the C2 site that showed the highest *f* value when a phenyl group was virtually incorporated. Given all these considerations, we envisioned the construction of a fluorescent library based on the novel furo[3,2-*e*]indolizine-based core skeleton with the R^1 group at the C6 position and the R^2 group at the C2 position. The R^1 and R^2 groups were diversified to phenyl moieties with an EDG and an EWG in order to investigate the effects of the electronic changes on the furoindolizine core skeleton. Additionally, our previous observation guided us to select the N8 position of the lactam ring as the linker site for further chemical conjugation because of the minimal perturbation of substituents at the N8 position towards their photophysical properties.[10a,c]

Based on the retrosynthetic analysis, the syntheses of the furo[3,2-*b*]pyridine derivatives[15] were a prerequisite for the fabrication of the furo[3,2-*e*]indolizine library (Scheme 1). We

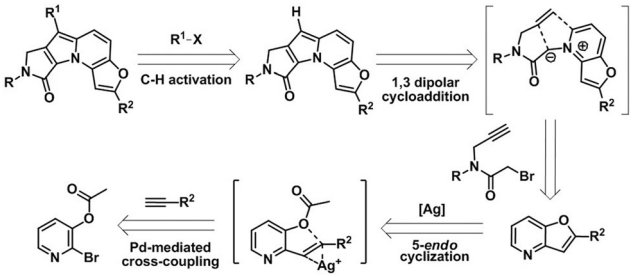

Scheme 1. Retrosynthetic analysis for the furoindolizine-based skeleton. [R = $(CH_2)_2$NHBoc].

incorporated the R^2-group-containing terminal acetylene moiety into 2-bromopyridin-3-yl acetate by Sonogashira coupling. After simple filtration of the resulting mixture, the silver-mediated cyclization allowed us to access the furo[3,2-*b*]pyridine derivatives in a facile manner. Then, the nucleophilic addition of furo[3,2-*b*]pyridine derivatives to alkyne-containing α-bromoamides yielded the furopyridinium salts as key intermediates. Without further purification, the resulting furopyridiniums were converted into furo[3,2-*e*]indolizine skeletons, aided by the treatment with 1,8-diazabicyclo[5.4.0]undec-7-ene (DBU) and CuI through a 1,3-dipolar cycloaddition. The R^1 functional groups were introduced at the last stage of the synthesis through direct C–H activation. After the optimization of reaction conditions (Table S2), the direct C–H activation of the furoindolizine core was successfully achieved through its thermal transformation in the presence of $PdCl_2(PPh_3)_2$, AgOAc, and KOAc at 100 °C in a 61–86 % yield with a moderate substrate scope, except for the electron-rich furoindolizine system **16** (see Table 1) because of its instability.

Using this synthetic route, we accomplished the synthesis of 15 furoindolizine-based fluorescent compounds and measured their photophysical properties, including their maximum absorption and emission wavelengths, molar absorptivity, and quantum yields (Table 1). We also calculated the oscillator strength *f* values of their S_0–S_1 transitions by TD-DFT calculations. We were particularly interested in the relationship of the observed molar absorptivity with the calculated *f* values on the basis of the ground-state-optimized geometry. Another theoretical value, the energy gap between the S_0 and S_1 states, was obtained through TD-DFT calculations to examine the predictable tendency of the emission-spectrum changes compared with the observed emission wavelengths.

 © 2015 Die Autoren. Veröffentlicht von Wiley-VCH Verlag GmbH & Co. KGaA, Weinheim

Table 1: A list of the compounds (cpd) in the furoindolizine library, with the values of their experimental and theoretical photophysical properties.

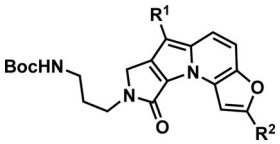

cpd	R^1	R^2	λ_{abs} [nm][a]	f[b]	ε[c]	E_{gap} [eV][d]	λ_{em} [nm][e]	Q.Y.[e]
01	H	H	355	0.2348	1.7E4	3.18	405	0.88
02	4-(CN)Ph	H	381	0.5467	2.2E4	2.90	453	0.69
03	Ph	H	372	0.3259	1.3E4	2.80	456	0.71
04	4-(NEt_2)Ph	H	386	0.2737	1.2E4	2.47	514	0.54
05	H	4-(CN)Ph	415	0.6262	2.4E4	2.61	502	0.85
06	4-(CN)Ph	4-(CN)Ph	434	0.9179	3.2E4	2.40	527	0.86
07	Ph	4-(CN)Ph	436	0.7117	2.5E4	2.34	533	0.80
08	4-(NEt_2)Ph	4-(CN)Ph	459	0.5137	1.9E4	1.98	630	0.10
09	H	Ph	391	0.5929	2.6E4	2.82	457	0.83
10	4-(CN)Ph	Ph	413	0.9641	3.9E4	2.60	491	0.83
11	Ph	Ph	410	0.6955	2.5E4	2.53	499	0.80
12	4-(NEt_2)Ph	Ph	424	0.5454	1.9E4	2.20	560	0.33
13	H	4-(NMe_2)Ph	405	0.9299	3.8E4	2.82	471	0.86
14	4-(CN)Ph	4-(NMe_2)Ph	431	1.1950	3.9E4	2.65	505	0.87
15	Ph	4-(NMe_2)Ph	423	1.0864	3.7E4	2.59	501	0.83
16	4-(NEt_2)Ph	4-(NMe_2)Ph	N/A	0.8915	N/A	2.28	N/A	N/A

All experimental data were obtained in dichloromethane (DCM). [a] Only the largest absorption maxima are shown. [b] Calculated oscillator strength values of the S_0–S_1 transition through TDDFT at the B3LYP/6-31G* level. [c] Molar absorption coefficient at the maximum absorption wavelength. [d] Calculated values of the energy gap between the S_0 and S_1 state based on the optimized geometry of first excited state through TDDFT at the B3LYP/6-31G* level. [e] Excited at the maximum absorption wavelength.

In terms of the molar absorptivity, the major enhancement was achieved through the additional π-conjugated systems at the R^2 position, in accordance with the trends predicted by their oscillator strength values (Figure 3a). Any aryl moiety at the R^2 position ensured the decent enhancement of the molar absorptivity, especially in the case of an electron-donating dimethylaminophenyl moiety (Figure 3b, bottom panel). For the R^1 position, however, effective enhancement of the molar absorptivity was achieved only via the incorporation of a 4-cyanophenyl group (Figure 3b, upper panel). In

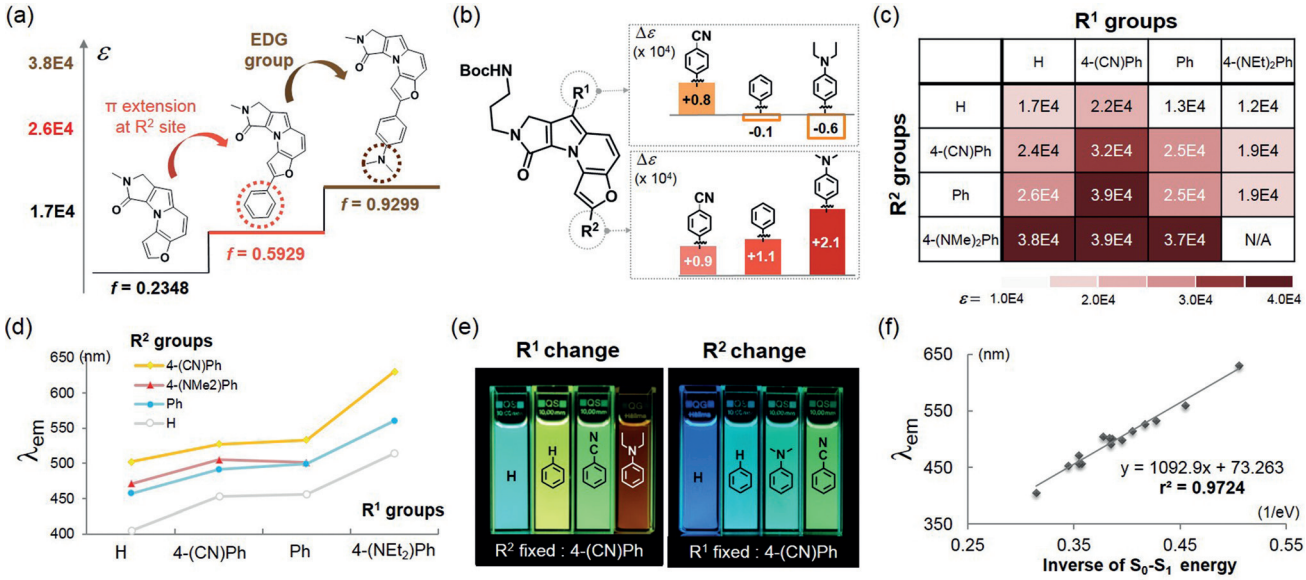

Figure 3. Emission- and absorption-related photophysical properties of the furoindolizine library. a) A schematic graph for the changes in oscillator strength values along with molar absorptivity upon structural modification. b) The average changes in the molar absorptivity upon the introduction of aryl moieties at the R^1 and R^2 positions in comparison with hydrogen. c) A colored table of the molar absorptivity of synthesized compounds. The darker colors represent higher molar absorptivity. d) Emission-wavelength changes depending on the R^1 and R^2 functional groups. e) Photographic images of the fluorescence emission colors of the representative compounds, irradiated at 365 nm. f) A scatter plot of the inverse of the S_0–S_1 energy gap versus the maximum emission wavelength.

 © 2015 Die Autoren. Veröffentlicht von Wiley-VCH Verlag GmbH & Co. KGaA, Weinheim

fact, a negligible change of the molar absorptivity or even its reduction was observed when we incorporated either a phenyl or aniline moiety at the R^1 position (Figure 3c). These contrasting events could possibly be attributed to the different effects of R^1 and R^2 groups on overlap efficiency between HOMO and LUMO;[16] an EDG at the R^1 position caused a localization of the electron density into the R^1 phenyl group in the HOMO, resulting in a lower spatial overlap between HOMO and LUMO (Figure S3a). An EDG at the R^2 position, however, extended their spatial overlap via a delocalization of the electron density into the furoindolizine core itself, allowing for efficient electron transition via light absorption (Figure S3b). Furthermore, we investigated the relationship between the observed molar absorptivity (ε) and the calculated oscillator strength value (f). To our pleasant surprise, a good linear relationship between ε and f was determined ($r^2 = 0.92$, Figure S4), suggesting both the effectiveness of our design strategy and the predictability of molar absorptivity. We also confirmed the predictability of molar absorptivity with the calculated f values in different organic fluorophores including BODIPY and coumarin (Figures S5 and S6).

Next, through the systematic comparison of the calculated energy gap between the S_0 and S_1 states with the observed emission wavelength, we observed interesting patterns in the furoindolizine system. As shown in Table 1, the longer emission wavelengths were observed when the furoindolizine compounds were equipped with an EDG at the R^1 and an EWG at the R^2 position. For example, for compounds sharing the same R^1 group, the change from a hydrogen to a 4-cyanophenyl group at the R^2 position caused a 90 nm bathochromic shift in the emission wavelength (Figure 3d). A more drastic bathochromic shift (over 110 nm on average) was observed in the case of 4-diethylaminophenyl moiety at the R^1 position, which was expected as a result of our initial design hypothesis. In addition, we were able to construct molecules covering a full visible-color range, spanning from 405 nm to 630 nm, with the furoindolizine library (Figure 3e). Moreover, we observed excellent correlation of the predicted emission wavelengths based on the theoretical S_0–S_1 energy gap with the observed emission wavelength ($r^2 = 0.97$), suggesting the feasibility of the emission-wavelength tuning of the furoindolizine analogs by simple calculations (Figure 3f).

As a proof of concept, our attention was directed toward the rational design of novel fluorescent molecules displaying desired photophysical properties, including emission wavelengths and enhanced molar absorptivity. In our previous reports, SF09, SF16, and SF20 were the brightest fluorophores that matched the fluorescence-filter sets for blue, green, and orange, respectively.[10b] On the basis of these SF analogs, we aimed to access brighter fluorescent compounds using the furoindolizine-based core skeleton. In fact, the brightness (B) of a fluorescence compound can be quantified by its molar absorptivity multiplied by its quantum yield. Therefore, we designed the novel furoindolizine analogs to possess enhanced molar absorptivity with the desired emission wavelengths, matched for each filter set. As shown in Figure 4a, we designed and synthesized a set of fluorophores (**17**, **18**, and

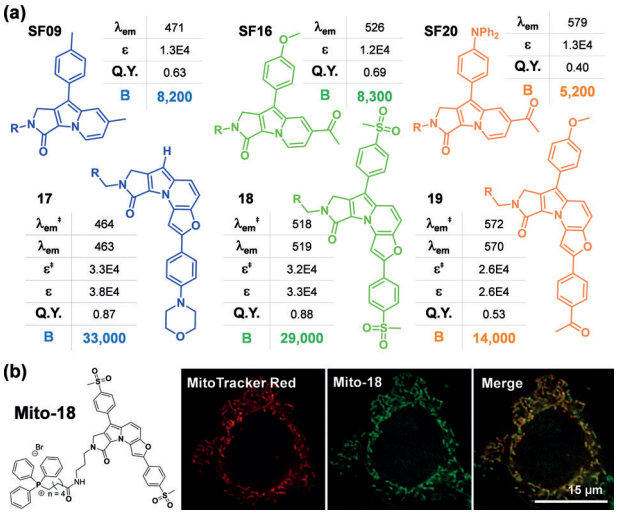

Figure 4. a) Rational design of novel furoindolizine-based fluorophores (**17**, **18**, and **19**) for each filter set of blue, green, and orange, respectively, with enhanced brightness in comparison with original SF analogs (SF09, SF16, and SF20). Estimated values (‡). [R = $(CH_2)_2NHBoc$] b) Chemical structure of **Mito-18** and fluorescent live cell images in HeLa human cervical cancer cells stained by MitoTracker Red and **Mito-18**.

19) with high accuracy and effectiveness on the basis of computable f values and energy gap (see the Supporting Information) and verified that the brightness of the newly designed organic fluorophores exhibited 4.0-, 3.5-, and 2.7-fold enhancements in blue-, green-, and orange-spectral areas, respectively. To demonstrate the applicability of newly developed furoindolizine-based fluorescent materials in biological systems, we designed a mitochondria probe, **Mito-18**, by incorporation of a triphenylphosphonium moiety at the N8 linker site (Figure 2b). As shown in Figure 4b, **Mito-18** exhibited an excellent sensitivity and selectivity toward mitochondria, confirmed by merged image with MitoTracker Red, in live cells, suggesting a reasonable solubility and stability of furoindolizine analogs as the potential monitoring tools in biomedical researches.

In summary, we developed a design strategy for the rational improvement of molar absorptivity of organic fluorophores guided by computable oscillator strength value. Using this strategy, we successfully discovered an unprecedented furo[3,2-*e*]indolizine-based fluorescent core skeleton from Seoul-Fluor with enhanced molar absorptivity. Through the synthesis of a series of furoindolizine analogs, we clearly showed that the computable values, such as the oscillator strength and the theoretical S_0–S_1 energy gap, can serve as excellent guideline for predicting the photophysical properties, such as the molar absorptivity and the emission wavelength. Moreover, our design capability was demonstrated by the rational discovery of three fluorescent dyes with matched emission wavelengths for each fluorescent filter set with significantly enhanced brightness and the subsequent application in live-cell imaging. This design strategy can be applied to the development of organic fluorophores and light-harvesting materials such as DSSC. In our previous reports,

 © 2015 Die Autoren. Veröffentlicht von Wiley-VCH Verlag GmbH & Co. KGaA, Weinheim

we successfully demonstrated the predictability of the emission wavelengths and quantum yields of the organic fluorophores. Now, we can rationally design brighter organic fluorophores via the enhancement of their molar absorptivity using calculated *f* values. Further in-depth mechanistic studies to reveal the origin of the relationship between structure and photophysical properties will be reported in due course.

Acknowledgements

This work was supported by the Creative Research Initiative (grant number 2014R1A3A2030423) and the Bio & Medical Technology Development Program (grant number 2012M3A9C4048780), funded by the National Research Foundation of Korea (NRF). Y.L. and A.J is grateful for a predoctoral BK21 plus scholarship.

Keywords: fluorescence · molar absorptivity · oscillator strength · photophysical properties · rational design

How to cite: *Angew. Chem. Int. Ed.* **2015**, *54*, 15689–15693
Angew. Chem. **2015**, *127*, 15915–15919

[1] a) B. Valeur, *Molecular Fluorescence: Principles and Applications*, Wiley-VCH, Weinheim, **2001**, p. 24–27; b) W. W. Parson, *Modern Optical Spectroscopy: With Examples from Biophysics and Biochemistry*, Springer, Berlin, Heidelberg, **2007**, p. 3, p. 91, p. 126.

[2] a) P. Wang, C. Klein, R. Humphry-Baker, S. M. Zakeeruddin, M. Grätzel, *J. Am. Chem. Soc.* **2005**, *127*, 808–809; b) F. Gao, Y. Wang, D. Shi, J. Zhang, M. Wang, X. Jing, R. Humphry-Baker, P. Wang, S. M. Zakeeruddin, M. Grätzel, *J. Am. Chem. Soc.* **2008**, *130*, 10720–10728; c) H. Chen, H. Huang, X. Huang, J. N. Clifford, A. Forneli, E. Palomares, X. Zheng, L. Zheng, X. Wang, P. Shen, B. Zhao, S. Tan, *J. Phys. Chem. C* **2010**, *114*, 3280–3286; d) X. Jiang, K. M. Karlsson, E. Gabrielsson, E. M. J. Johansson, M. Quintana, M. Karlsson, L. Sun, G. Boschloo, A. Hagfeldt, *Adv. Funct. Mater.* **2011**, *21*, 2944–2952.

[3] a) J. S. Melinger, Y. Pan, V. D. Kleiman, Z. Peng, B. L. Davis, D. McMorrow, M. Lu, *J. Am. Chem. Soc.* **2002**, *124*, 12002–12012; b) Q. Yu, S. Liu, M. Zhang, N. Cai, Y. Wang, P. Wang, *J. Phys. Chem. C* **2009**, *113*, 14559–14566; c) Y. Lin, P. Cheng, Y. Liu, Q. Shi, W. Hu, Y. Li, X. Zhan, *Org. Electron.* **2012**, *13*, 673–680.

[4] a) J. Chen, A. Burghart, A. Derecskei-Kovacs, K. Burgess, *J. Org. Chem.* **2000**, *65*, 2900–2906; b) W. Zhao, E. M. Carreira, *Chem. Eur. J.* **2006**, *12*, 7254–7263; c) S. Goeb, R. Ziessel, *Org. Lett.* **2007**, *9*, 737–740; d) N. Karton-Lifshin, L. Albertazzi, M. Bendikov, P. S. Baran, D. Shabat, *J. Am. Chem. Soc.* **2012**, *134*, 20412–20420; e) K. Nakanishi, D. Fukatsu, K. Takaishi, T. Tsuji, K. Uenaka, K. Kuramochi, T. Kawabata, K. Tsubaki, *J. Am. Chem. Soc.* **2014**, *136*, 7101–7109.

[5] a) E. Kim, S. B. Park, *Chem. Asian J.* **2009**, *4*, 1646–1658; b) H. Kobayashi, M. Ogawa, R. Alford, P. L. Choyke, Y. Urano, *Chem. Rev.* **2010**, *110*, 2620–2640; c) S.-W. Yun, N.-Y. Kang, S.-J. Park, H.-H. Ha, Y. K. Kim, J.-S. Lee, Y.-T. Chang, *Acc. Chem. Res.* **2014**, *47*, 1277–1286.

[6] a) L. D. Lavis, R. T. Raines, *ACS Chem. Biol.* **2008**, *3*, 142–155; b) L. D. Lavis, R. T. Raines, *ACS Chem. Biol.* **2014**, *9*, 855–866.

[7] R. C. Hilborn, *Am. J. Phys.* **1982**, *50*, 982–986.

[8] a) R. C. Evans, P. Douglas, H. D. Burrow, *Applied Photochemistry*, Springer, Berlin, **2013**, p. 60; b) S. Ji, J. Yang, Q. Yang, S. Liu, M. Chen, J. Zhao, *J. Org. Chem.* **2009**, *74*, 4855–4865; c) X. Zhang, Y. Xiao, J. Qi, J. Qu, B. Kim, X. Yue, K. D. Belfield, *J. Org. Chem.* **2013**, *78*, 9153–9160.

[9] a) H. Sahu, A. N. Panda, *Macromolecules* **2013**, *46*, 844–855; b) A. M. Sand, C. Liu, A. J. S. Valentine, D. A. Mazziotti, *J. Phys. Chem. A* **2014**, *118*, 6085–6091.

[10] a) E. Kim, M. Koh, J. Ryu, S. B. Park, *J. Am. Chem. Soc.* **2008**, *130*, 12206–12207; b) E. Kim, M. Koh, B. J. Lim, S. B. Park, *J. Am. Chem. Soc.* **2011**, *133*, 6642–6649; c) Y. Lee, S. Na, S. Lee, N. L. Jeon, S. B. Park, *Mol. Biosyst.* **2013**, *9*, 952–956; d) E. J. Choi, E. Kim, Y. Lee, A. Jo, S. B. Park, *Angew. Chem. Int. Ed.* **2014**, *53*, 1346–1350; *Angew. Chem.* **2014**, *126*, 1370–1374; e) E. Kim, Y. Lee, S. Lee, S. B. Park, *Acc. Chem. Res.* **2015**, *48*, 538–547.

[11] a) E. Kim, S. Lee, S. B. Park, *Chem. Commun.* **2012**, *48*, 2331–2333; b) E. J. Choi, S. B. Park, *Org. Biomol. Chem.* **2015**, *13*, 5202–5208.

[12] a) J.-L. Lim, S. Chirayil, R. P. Thummel, *J. Org. Chem.* **1991**, *56*, 1492–1500; b) Y. Liang, P. Zhang, S. Yang, Z. Tao, J. Chen, *Adv. Energy Mater.* **2013**, *3*, 600–605; c) D. Dang, M. Xiao, P. Zhou, J. Zhong, J. Fan, N. Su, W. Xiong, C. Yang, Q. Wang, Y. Wang, Y. Pei, R. Yang, W. Zhu, *Eur. J. Org. Chem.* **2015**, *2015*, 820–827; d) S.-I. Kato, T. Furuya, M. Nitani, N. Hasebe, Y. Ie, Y. Aso, T. Yoshihara, S. Tobita, Y. Nakamura, *Chem. Eur. J.* **2015**, *21*, 3115–3128; e) J.-D. Huang, S. Chai, H. Ma, B. Dong, *J. Phys. Chem. C* **2015**, *119*, 33–44.

[13] a) K. Umezawa, Y. Nakamura, H. Makino, D. Citterio, K. Suzuki, *J. Am. Chem. Soc.* **2008**, *130*, 1550–1551; b) K. Umezawa, A. Matsui, Y. Nakamura, D. Citterio, K. Suzuki, *Chem. Eur. J.* **2009**, *15*, 1096–1106.

[14] K. Higashiguchi, K. Matsuda, Y. Asano, A. Murakami, S. Nakamura, M. Irie, *Eur. J. Org. Chem.* **2005**, *2005*, 91–97.

[15] a) A. Chartoire, C. Comoy, Y. Fort, *Tetrahedron* **2008**, *64*, 10867–10873; b) A. Jasselin-Hinschberger, C. Comoy, A. Chartoire, Y. Fort, *Eur. J. Org. Chem.* **2015**, *2015*, 2321–2331.

[16] a) D. Cai, M. A. L. Marques, B. F. Milne, F. Nogueira, *J. Phys. Chem. Lett.* **2010**, *1*, 2781–2787; b) X. Liu, Z. Xu, J. M. Cole, *J. Phys. Chem. C* **2013**, *117*, 16584–16595.

Received: July 13, 2015
Revised: September 12, 2015
Published online: November 13, 2015

 © 2015 Die Autoren. Veröffentlicht von Wiley-VCH Verlag GmbH & Co. KGaA, Weinheim